



OPEN The histone acetyl transferases CBP and p300 regulate stress response pathways in synovial fibroblasts at transcriptional and functional levels

Monika Krošelj^{1,2,3}, Marcel Gabathuler¹, Larissa Moser¹, Malgorzata Maciukiewicz^{1,4,5}, Thomas Züllig¹, Tanja Seifritz¹, Matija Tomšič^{2,3}, Oliver Distler¹, Caroline Ospelt¹ & Kerstin Klein^{4,5}✉

The activation of stress response pathways in synovial fibroblasts (SF) is a hallmark of rheumatoid arthritis (RA). CBP and p300 are two highly homologous histone acetyl transferases and writers of activating histone 3 lysine 27 acetylation (H3K27ac) marks. Furthermore, they serve as co-factors for transcription factors and acetylate many non-histone proteins. Here we showed that p300 but not CBP protein expression was down regulated by TNF and 4-hydroxynonenal, two factors that mimic inflammation and oxidative stress in the synovial microenvironment. We used existing RNA-sequencing data sets as a basis for a further in-depth investigation of individual functions of CBP and p300 in regulating different stress response pathways in SF. Pathway enrichment analysis pointed to a profound role of CBP and/or p300 in regulating stress response-related gene expression, with an enrichment of pathways associated with oxidative stress, hypoxia, autophagy and proteasome function. We silenced CBP or p300, and performed confirmatory experiments on transcriptome, protein and functional levels. We have identified some overlap of CBP and p300 target genes in the oxidative stress response pathway, however, with several genes being regulated in opposite directions. The majority of stress response genes was regulated by p300, with a specific function of p300 in regulating hypoxia response genes and genes encoding proteasome subunits. Silencing of p300 suppressed proteasome enzymatic activities. CBP and p300 regulated autophagy on transcriptome and functional levels. Whereas CBP was indispensable for autophagy synthesis, silencing of p300 affected late-stage autophagy. In line with impaired autophagy and proteasome function, poly-ubiquitinated proteins accumulated after silencing of p300.

The activation of stress response pathways is an early event in joints of patients with rheumatoid arthritis (RA). In particular, adaption to hypoxia and oxidative stress, autophagy, the unfolded protein response (UPR) and the endoplasmic reticulum (ER) stress response are activated pathways in the RA synovium^{1–6}.

Synovial fibroblasts (SF) are the key joint resident cells that create a joint-specific microenvironment⁷ and drive joint destruction and inflammation in RA⁸. Furthermore, SF promote angiogenesis by producing vascular endothelial growth factor (VEGF)⁸. The neovascular network is dysfunctional, rendering the synovial tissue hypoxic. Hypoxia and subsequent oxidative stress within the RA joint significantly contribute to the activation of SF and induce a metabolic switch from oxidative phosphorylation towards glycolysis⁹. This is associated with an increased invasive behavior and proliferation of SF, and the secretion of chemotactic factors that lead to migration of inflammatory cells^{1,10}. The upregulation of metabolic and stress response genes was described as a characteristic of SF in chronic versus acute inflammation in a mouse model upon repeated exposure to inflammatory stimuli¹¹.

¹Center of Experimental Rheumatology, Department of Rheumatology, University Hospital Zurich, University of Zurich, Zurich, Switzerland. ²Department of Rheumatology, University Medical Centre Ljubljana, Ljubljana, Slovenia. ³Faculty of Medicine, University of Ljubljana, Ljubljana, Slovenia. ⁴Department of BioMedical Research, University of Bern, Murtenstrasse 28, 3008 Bern, Switzerland. ⁵Department of Rheumatology and Immunology, Inselspital, Bern University Hospital, Bern, Switzerland. ✉email: kerstin.klein@unibe.ch

Upstream regulatory factors that integrate the stress and inflammatory response in RA SF have not been investigated yet in detail. CREB-binding protein (CBP) and p300 are two highly homologous enzymes with histone acetyltransferase (HAT) activities. They are often considered as proteins with identical functions (referred as CBP/ p300) and few studies address their individual roles^{12–14}. CBP/ p300 are widely studied as writers of the activating histone mark histone 3 lysine 27 acetylation (H3K27ac) but many non-histone proteins are among their targets, including several transcription factors^{15,16}. We have recently studied individual functions of CBP and p300 in regulating the inflammatory response of SF¹⁴. We have identified p300 as the major HAT in SF that possessed overlapping and distinct target genes and functions with CBP¹⁴.

Here we focused on the regulation of CBP and p300 expression and their individual roles in regulating stress response pathways in SF. We used existing transcriptome analysis of unstimulated and TNF-stimulated SF silenced for CBP or p300, respectively. We performed an in-depth analysis on their contribution in regulating different stress response pathways in SF and performed confirmatory experiments on RNA, protein and functional levels.

Results

p300 expression is suppressed by TNF and oxidative stress

To study CBP and p300 regulation, we have treated SF with the lipid peroxidation products 4-HNE to mimic oxidative stress¹⁷, in absence and presence of TNF. Whereas 4-HNE and TNF did not induce any consistent effects on the expression of CBP, the expression of p300 was suppressed by TNF by 52.1% ($\pm 13.2\%$) and was even further down regulated in presence of TNF and 4-HNE by 60.7% ($\pm 18.0\%$) (Fig. 1a, b, supplementary Fig. 1). In addition, the expression of p300 but not CBP was dose-dependently suppressed by H₂O₂ (supplementary Fig. 2). To study individual functions of CBP and p300, we followed a silencing strategy for both enzymes, enabling us to compare the effects of p300 to those of CBP. Our results on p300 regulation suggest, that the silencing approach for studying p300 function, resembled p300 expression in SF under conditions of oxidative stress and inflammation (Fig. 3d).

CBP and p300 regulate stress response pathways in SF

We used existing RNAseq data sets¹⁴ from knee and hand SF that were silenced for CBP and p300 in absence and presence of TNF (Fig. 2a, d) as a basis to study individual functions of CBP and p300 in SF¹⁴ in regulating stress response pathways. In addition to our previously reported functions of CBP and p300 in regulating inflammatory pathways in SF, our pathway analysis of differentially expressed genes (DEG) in RNAseq data sets revealed an enrichment of target genes in a variety of stress response pathways (Fig. 2, Supplementary table 2). In line with p300 being the major writer of H3K27ac marks in SF¹⁴, the number of stress response pathways that we identified in SF silenced for p300 exceeded those identified in SF silenced for CBP. The majority of stress pathways regulated by CBP was associated with a prevention of DNA damage, such as “response to ionizing radiation”, “regulation of response to DNA damage stimulus”, “double-strand break repair”, “cellular response to UV, oxidative stress or chemical stress” (Fig. 2b, c; supplementary table 2). All of these pathways were additionally found to be regulated by p300. Among the pathways that were specifically regulated by p300 were the “response to hypoxia and oxygen levels”, as well as pathways associated with protein homeostasis, such as “autophagy”, “proteasomal pathways” and the response to “endoplasmic reticulum (ER) stress” (Fig. 2e, f; supplementary table 2). To evaluate our key findings from the pathway analysis, we performed a set of confirmatory experiments and measured the expression of selected genes on RNA and protein levels, and evaluated functional consequences induced by DEG.

The oxidative stress response is co-regulated by CBP and p300

Oxidative stress response is an early event in the synovium of patients with RA¹⁸. We have identified the “cellular response to oxidative stress” as a shared stress pathway that was enriched in CBP and in p300 target genes in unstimulated and in TNF-stimulated SF (Fig. 3a). In both conditions, the majority of target genes in this

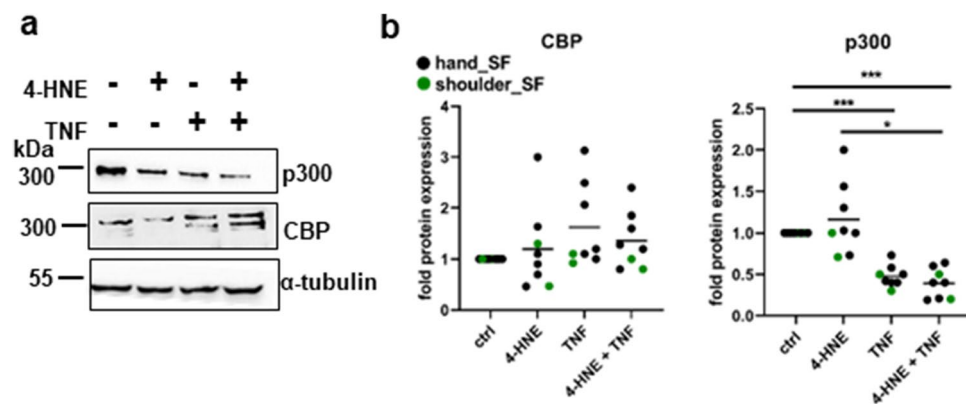


Figure 1. Regulation of CBP and p300 protein expression. (a) Representative Western blot and (b) densitometric analysis of SF ($n=8$) treated with 4-HNE and TNF, or a combination of both. Full length blots are shown in supplementary Fig. 1 * $p < 0.05$, *** $p < 0.005$.

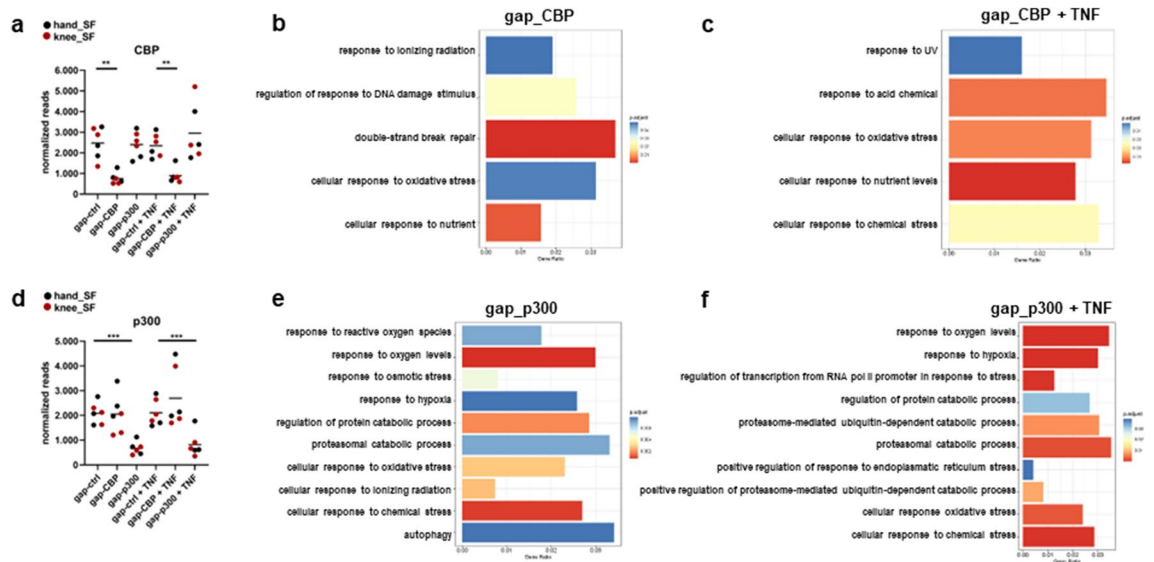


Figure 2. CBP and p300 target genes are enriched in stress response pathways. Transcriptomes were determined by RNAseq¹⁴. Normalized reads confirming the silencing of (a) CBP and (d) p300. Significantly affected genes (\pm fold change > 1.5, FDR < 0.05) entered pathway enrichment analysis for Gene Ontology (GO) biological process (BP). Enriched GO BP identified after silencing of (b) CBP and (e) p300 in absence and (c) and (f) presence of TNF. Details on displayed pathways are shown in supplementary table 2. ** $p < 0.01$, *** $p < 0.005$.

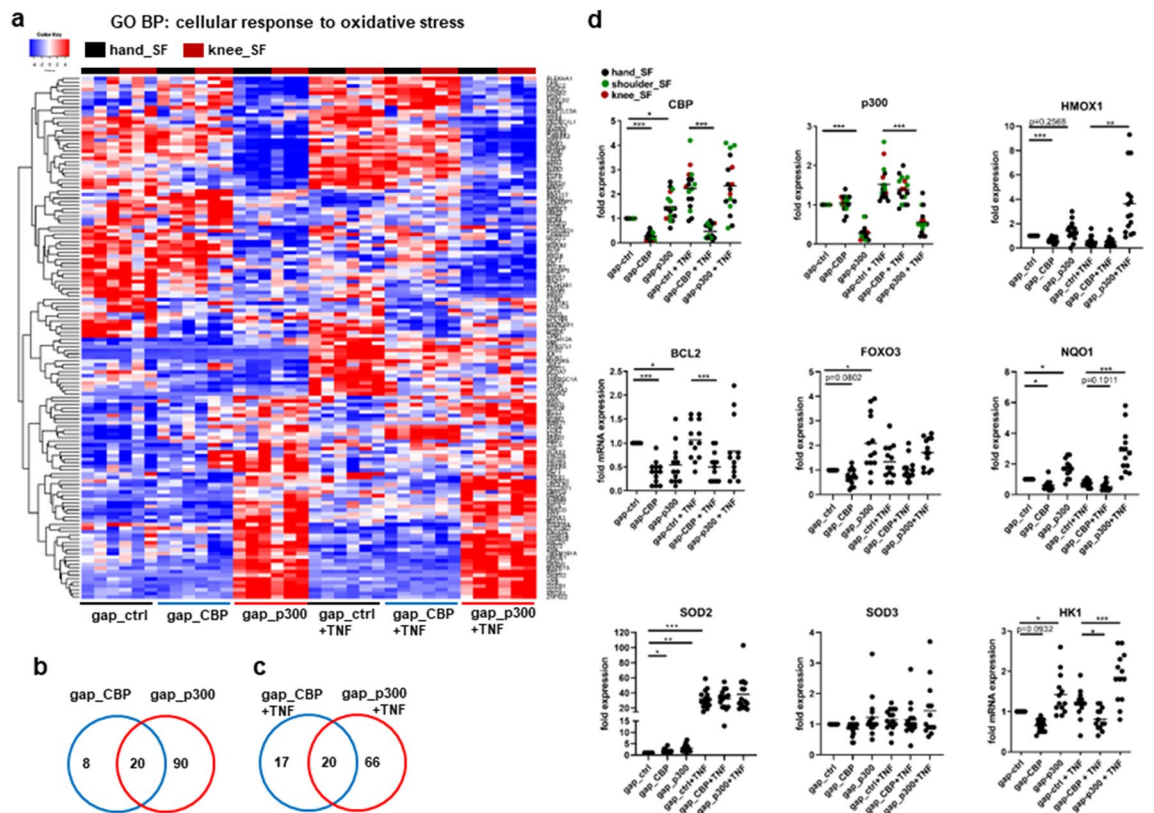


Figure 3. CBP and p300 regulate the response to oxidative stress. (a) Heatmap of DEG (\pm fold change > 1.5, FDR < 0.05) enriched in the biological process (BP) “cellular response to oxidative stress” that were identified by RNAseq of SF silenced for CBP or p300. Venn diagrams indicating the number of genes regulated by CBP and p300 in (b) unstimulated and (c) in TNF-stimulated SF. (d) Changes in mRNA expression for selected DEG were analyzed by Real-time PCR in an independent cohort of samples (n = 13–15) from data shown in (a). Results on mRNA expression of these in genes in SF from different joints (hand, shoulder, knee) are shown in supplementary Fig. 3. * $p < 0.05$, ** $p < 0.01$, *** $p < 0.005$.

pathway was regulated by p300, with 8.8% and 14.6% of genes being co-regulated by CBP (Fig. 3b, c). Among the 20 overlapping DEG identified in unstimulated SF were the apoptosis regulator BCL2, NAD(P)H quinone dehydrogenase 1 (NQO1), and the transcription factor forkhead box O3 (FOXO3). In TNF-stimulated SF, we identified additionally superoxide dismutase (SOD) 3 as a shared target gene of CBP and p300. We selected some DEG for validating the effects of CBP and p300 silencing on mRNA expression levels in an independent set of samples (Fig. 3d). Silencing reduced the expression of CBP mRNA by 73.6% ($\pm 14.6\%$) and 78.9% ($\pm 28.2\%$) in unstimulated and TNF-stimulated SF, respectively, and did not reduce the expression of p300. Silencing of p300 reduced the expression of p300 by 71.8% ($\pm 18.1\%$) and 63.2% ($\pm 30.2\%$), respectively, and did not reduce the expression of CBP (Fig. 3d). Silencing efficiency was similar in SF from hand, shoulder and knee SF. Similar effects of CBP and p300 silencing were only identified on the expression of BCL2 and SOD2. Silencing of CBP and p300 reduced the expression of BCL2 in unstimulated SF. In TNF-stimulated SF, p300 suppressed the expression of BCL2 only in knee SF ($n = 3$, supplementary Fig. 3). The expression of SOD2 was induced by silencing of CBP and p300 in unstimulated SF (Fig. 3d). CBP reduced the expression of SOD3 ($p = 0.0674$) only in SF from shoulders ($n = 5$) and knee ($n = 3$) but had no effect on hand SF (supplementary Fig. 3). We have detected opposing effects of CBP and p300 in regulating the expression of FOXO3, hexokinase (HK) 1, NQO1 and heme oxygenase 1 (HMOX1) (Fig. 3d). Whereas silencing of CBP suppressed the expression of these genes, silencing of p300 increased their expression. This suggests that CBP and p300 have opposing functions in regulating of oxidative stress response, at least in a subset of genes.

CBP and p300 regulate autophagy

Our pathway analysis of DEG pointed to a role of p300 in the regulation of protein catabolism, including pathways associated with autophagy and the proteasome. Oxidative stress and hypoxia play a pivotal role in the pathogenesis of RA¹⁸ and are known inducers of autophagy¹⁹. We have identified p300 as a major factor that regulates not only oxidative stress response but also genes enriched in the “response to hypoxia” and “response to oxygen” levels (supplementary Fig. 4). Among the p300 target genes, were the metabolic enzymes HK2 and pyruvate dehydrogenase alpha 1 (PDHA1), the prolyl hydroxylase EGLN2, the pro-angiogenic factor VEGF, and the transcription factor peroxisome proliferator-activated receptor gamma (PPARG).

In line with their HAT-dependent regulation, we have detected high levels of H3K27ac in the genomic regions surrounding the transcription start sites of autophagy related (ATG)5, ATG7, ATG16L1, and the autophagy regulator histone deacetylase 6 (HDAC6) (Fig. 4a). Silencing of p300 decreased basal levels of ATG7, and increased levels ATG5 in TNF-treated SF, as well as ATG16L1 levels in untreated and TNF-treated SF (Fig. 4b). CBP silencing had the same effect on ATG5 and ATG16L1 in TNF-treated SF, but did not affect their expression in unstimulated SF. Both silencing of CBP and p300 decreased the expression of HDAC6 in unstimulated SF. Upon TNF-stimulation, HDAC6 was only decreased by silencing of CBP or p300 in SF from shoulder and knee but not in SF from hand (supplementary Fig. 5). To functionally test potential changes in autophagy activity, we performed Western blotting using LC3B conversion and p62 protein expression as autophagy markers in presence and absence of the lysosomal inhibitor bafilomycin A1 (Fig. 4c–e, supplementary Fig. 6). Silencing of CBP reduced the conversion of LC3B and the protein expression of p62 in presence and absence of TNF. Results were similar in presence of bafilomycin A1, indicating a decrease in autophagosome synthesis. In contrast, the conversion of LC3B and p62 expression were increased after silencing of p300 in unstimulated SF, indicating increased autophagy. This effect was lost for LC3B after treatment with TNF, and LC3B conversion was even decreased in presence of bafilomycin A1. This indicates a late-stage block of autophagy after silencing of p300 in TNF-stimulated SF.

p300 silencing affects proteasome activity

Our pathway analysis of DEG suggested a pivotal and specific role of p300 in regulating proteasome function (supplementary table 2). We have detected an increased expression of the majority of genes encoding for proteasome machinery components after silencing of p300 (Fig. 5a), which were enriched in the pathways “proteasomal protein catabolic process” and “proteasome-mediated ubiquitin-dependent protein catabolic process”. Silencing of CBP had no effect on the expression of these genes (Fig. 5a). Our functional analysis of the proteasome enzymatic activities revealed that silencing of p300 suppressed the chymotrypsin-like and trypsin-like activities, whereas the caspase-like enzymatic activity was not affected (Fig. 5b). These data suggest that the increased expression of proteasome-related genes on mRNA levels was compensatory for the decreased enzymatic activities after silencing of p300. In line with decreased enzymatic proteasome activities, we have detected an increased accumulation of poly-ubiquitinated proteins in SF that were silenced for p300, in particular in samples that were stimulated with TNF. This was effect was not detected in SF after silencing of CBP (Fig. 5c).

Discussion

Hypoxia, the formation of reactive oxygen species (ROS), and subsequent oxidative stress in synovial tissues are key events in the pathogenesis of RA¹. We provide here evidence that CBP and p300 are pivotal regulators of the adaptive response of SF that integrate the cell’s transcriptional and functional regulation of stress response pathways.

CBP and p300 are HATs and writers of H3K27ac marks, activating post-translational histone modifications present in enhancers and promoters²⁰. Among the CBP/ p300 target proteins are beside histones several non-histone proteins, including many transcription factors and signaling effectors^{16,21}. Despite their high protein sequence homology, CBP and p300 have several individual functions, identified by our own and other studies^{12–14}.

In SF, a sustained H3K27ac in inflammatory gene promoters was associated with a prolonged and persistent expression of the corresponding genes²². We have recently shown that p300 is the major HAT in SF that exerts

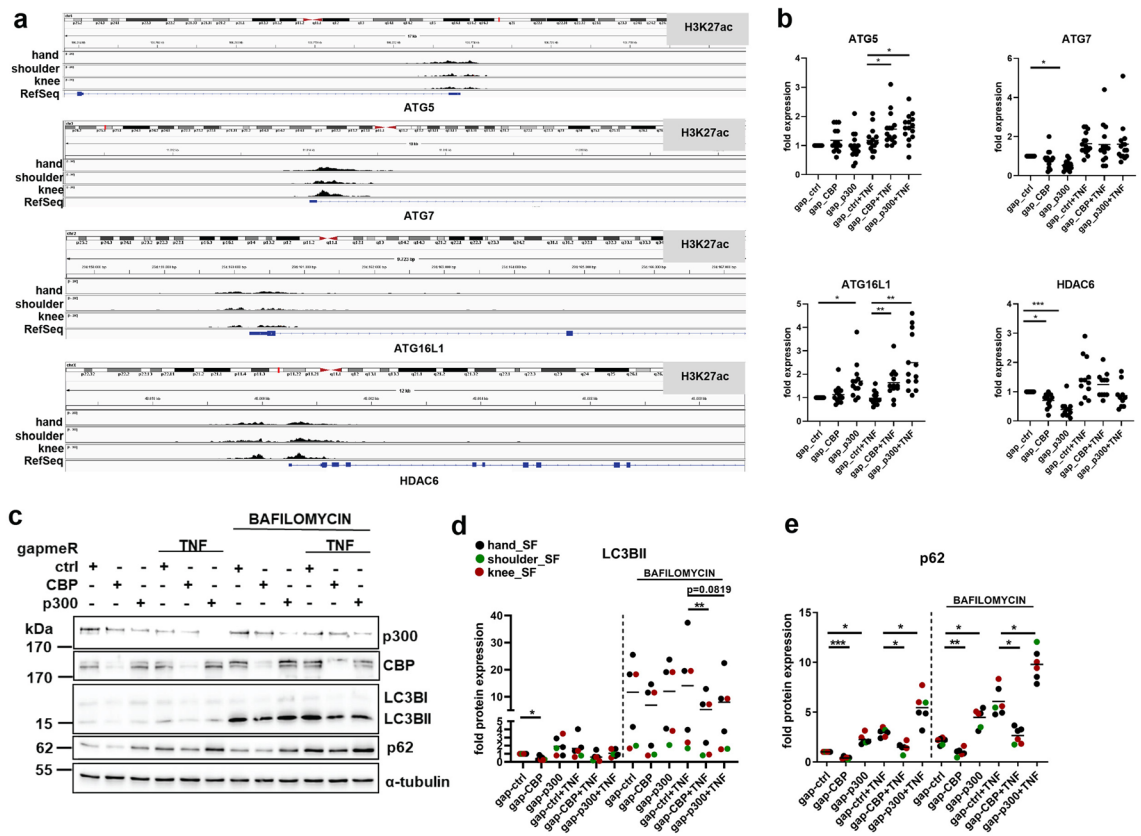


Figure 4. CBP and p300 regulate autophagy. **(a)** ChIPseq analysis of H3K27ac marks in the *ATG5*, *ATG7*, *ATG16L1* and *HDAC6* genetic loci up- and downstream of the transcription start sites in hand, shoulder and knee SF. **(b)** Changes in mRNA expression for selected autophagy-related genes were analyzed by Real-time PCR in an independent cohort (n = 12–15) of samples used for RNAseq. Results on mRNA expression of these in genes in SF from different joints (hand, shoulder, knee) are shown in supplementary Fig. 5. **(c)** Representative Western blots and densitometric analysis of **(d)** LC3B (n = 6) and **(e)** p62 (n = 6). Markers of autophagy were analysed in absence and presence of bafilomycin A1 to assess the autophagix flux. Full length blots are shown in supplementary Fig. 6. * $p < 0.05$, ** $p < 0.01$, *** $p < 0.005$.

pro- and anti-inflammatory roles. This is contrast to CBP, that exerted anti-inflammatory effects upon silencing, and specifically regulated TNF-induced interferon signature gene expression¹⁴. Although we have ruled out that silencing of p300 additionally decreased CBP and vice versa, we cannot completely rule out other potential off target effects following our silencing approach. *Krosel et al.* have shown that inhibitors targeting the HAT or bromodomain of CBP/ p300 to a large extent resemble effects of p300 silencing, including an increased expression of TNF-induced pro-inflammatory gene expression¹⁴.

Our RNAseq data provides evidence that numbers of p300-regulated target genes exceed those of CBP-regulated target genes also in terms of stress response. Whereas the cellular response to oxidative stress and autophagy were co-regulated by CBP and p300, genes associated with a response to oxygen levels, hypoxia and pathways associated with proteasome regulation and function were specifically enriched after silencing of p300. In pathways that were co-regulated by CBP and p300, we have identified several genes that were regulated in opposite directions. These results point to individual functions of the two enzymes on target genes levels, similarly to what we have already observed for many inflammatory genes¹⁴. In addition, a small number of measured CBP and p300 target genes, namely *BCL2*, *SOD3*, and *HDAC6*, might be regulated in a joint-specific manner, as indicated by our Real-time PCR results in a limited number of samples for each joint location. *Frank-Bertoncelj et al.* have previously shown that H3K27ac is one of the mechanisms controlling the joint-specific expression of homeobox (HOX) transcription factors in SF from different locations⁷. To draw a final conclusion whether stress-associated target genes are regulated in a joint-specific manner, larger numbers of SF from different joints would be needed, along with H3K27ac ChIPseq data in unstimulated and TNF-stimulated SF from different joints.

In addition to different roles of CBP and p300 in regulating target gene expression, we showed here a differential regulation of CBP and p300 by stimulating SF with 4-HNE and TNF (Fig. 6). These factors are present in the synovial microenvironment in RA, and mimic the oxidative stress and inflammation, respectively. Whereas 4-HNE and TNF, similarly to H_2O_2 , suppressed the expression of p300, CBP was not affected. 4-HNE is a lipid peroxidation product generated upon increased levels of ROS. Levels of 4-HNE are elevated in serum, synovial fluids and synovial tissues of RA patients, and serum levels of 4-HNE correlate with the structural damage such as erosions in the early stage of RA^{23,24}. As mimicked by our silencing approach, the TNF- and 4-HNE-mediated

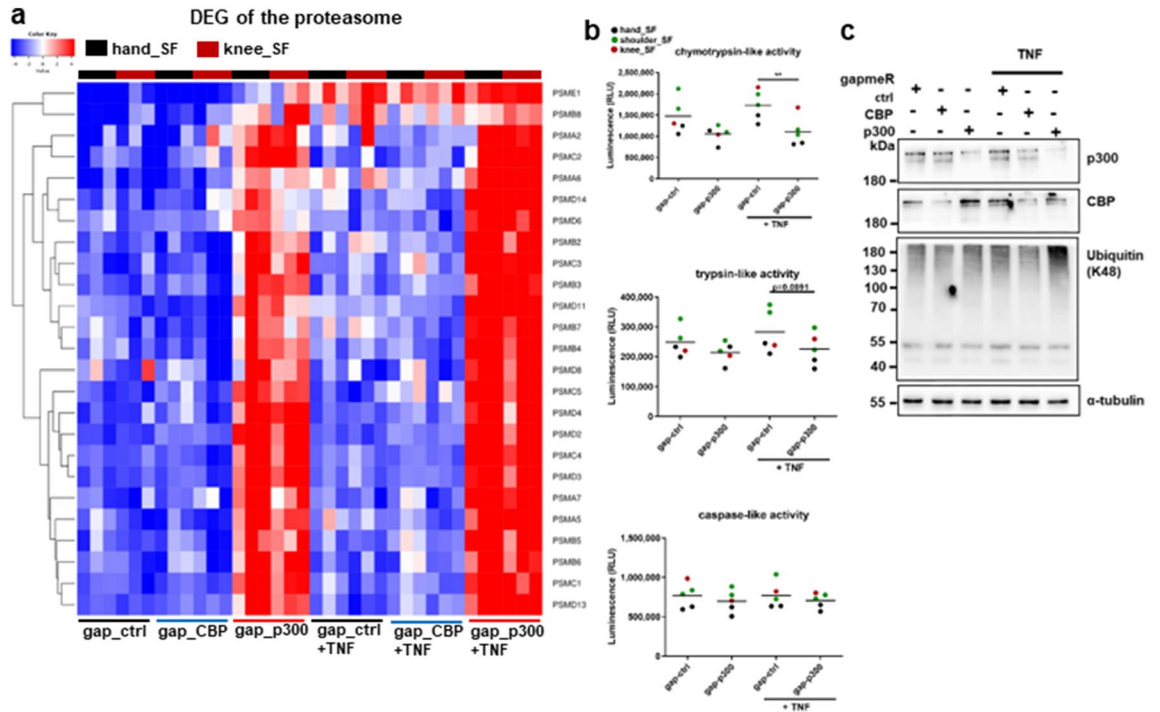


Figure 5. p300 regulates the expression and activity of proteasomal components. (a) Heatmap of DEG (\pm fold change > 1.5 , FDR < 0.05) encoding components of the proteasome, and selected from the enriched biological processes (BP) “proteasomal protein catabolic process” and “proteasome-mediated ubiquitin-dependent protein catabolic process”. (b) Chymotrypsin-like, trypsin-like and caspase-like proteasome activities in SF ($n = 5$) silenced for p300 in absence and presence of TNF. (c) The accumulation of poly-ubiquitinated proteins in SF silenced for CBP and p300, respectively, was analysed by Western blotting. A representative Western blot is shown ($n = 4$). Full length blots are shown in supplementary Fig. 7 $**p < 0.01$.

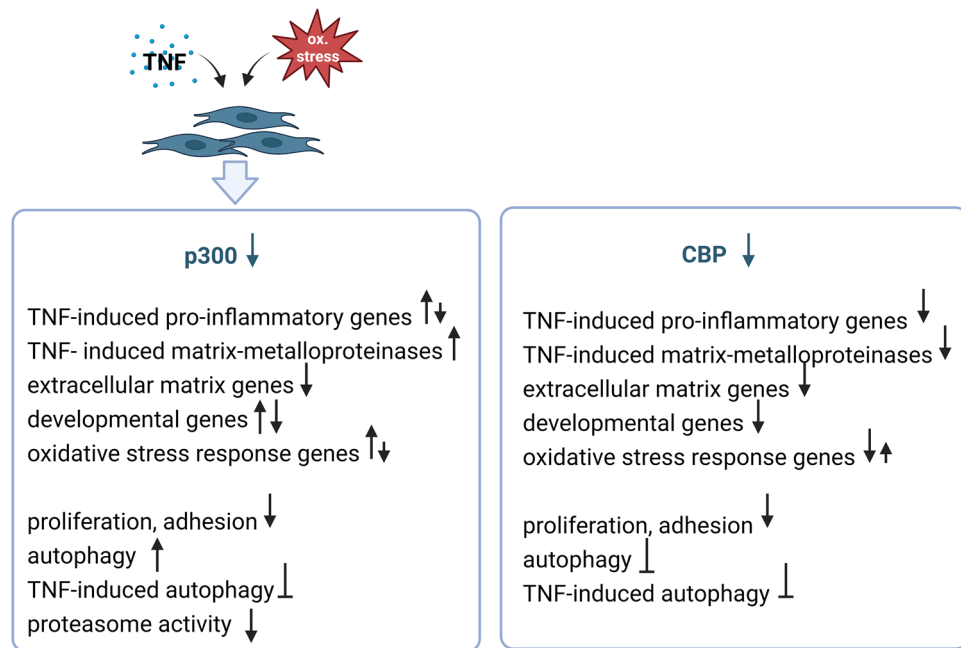


Figure 6. Summary of CBP- and p300-regulated pathways in SF. The expression of p300 but not of CBP is down regulated in synovial fibroblasts upon exposure to TNF and oxidative stress. Effects of p300 and CBP silencing are shown based on findings from this and a previous study¹⁴. Down facing arrows indicate suppressed expression or function, up facing arrows indicate increased expression or function. The figure was created by BioRender.com.

suppression of p300 expression in the synovial RA microenvironment has fundamental consequences on SF behaviour. Our data sets from the previous¹⁴ and the current study indicate that a decreased expression of p300 was associated with an increased expression of many inflammatory cytokines, chemokines matrix metalloproteinases, and stress response genes in SF. Among these genes were HK2, a marker indicating the metabolic switch of SF towards glycolysis, and VEGF, a pro-angiogenic factor secreted to overcome hypoxia¹.

TNF stimulation of SF was shown to induce markers of endoplasmic reticulum (ER) stress and autophagy²⁵. Our data suggest that CBP and p300 regulate autophagy at transcriptional level and effects autophagic flux. The assessment of autophagy in presence of the lysosomal inhibitor bafilomycin A1 indicated that CBP and p300 regulate autophagy function at different stages within the autophagic process. CBP silencing affected autophagosome synthesis. In contrast, silencing of p300 induced autophagy in unstimulated SF, and induced a late-stage block of autophagy in TNF-stimulated SF, a condition in which poly-ubiquitinated proteins in SF accumulated. Accordingly, silencing of p300 only increased cell death in presence of TNF, as indicated previously¹⁴. *Kato et al.* have previously shown that autophagy induction partially compensated for an impaired clearance of poly-ubiquitinated proteins in SF after blocking proteasome function, pointing to a protective effect of autophagy induction in SF in such conditions⁵. Here we observed a similar compensatory mechanism after silencing of p300, which was associated with a suppression of proteasome enzymatic activities and an induction of autophagy. This finding is in line with a previous study in HeLa cells in which the knockdown of p300 was associated with a decreased acetylation of autophagy-related proteins and increased levels of autophagy²⁶.

Acetylation and deacetylation of components of the autophagy machinery control all steps of this catabolic process from autophagosome initiation to LC3 conjugation, cargo assembly and autophagosome-lysosome fusion^{27,28}. Different classes of acetyltransferases, including CBP and p300, and deacetylases, including sirtuin1, HDAC4 and HDAC6 are involved in the regulation of autophagy^{27,29}. In addition, the function of autophagy-related transcription factors, such as transcription factor EB (TFEB), Foxo1 and Foxo3, are regulated by deacetylation^{28,30}. The increased translation of FOXO3 mRNA has recently been described to facilitate autophagy initiation³¹. We showed here that in unstimulated SF, FOXO3 mRNA was increased upon silencing of p300, a condition in which autophagic flux was increased. HDAC6 binds to poly-ubiquitinated proteins in SF²⁹, and promotes autophagy by facilitating autophagosome-lysosome fusion²⁷. On the other hand, HDAC6 was also shown to suppress autophagy by deacetylating TFEB and Foxo1³⁰. This might explain the inverse regulation of HDAC6 and ATG5 and ATG16L1 in SF.

A global analysis of the CBP/ p300-dependent acetylome in mouse embryonic fibroblasts (MEF) suggested that also proteasome functions might be regulated by these enzymes²¹. The majority of components of the proteasome machinery exhibited numerous CBP/ p300-dependent acetylation sites in regulatory and enzymatic subunits in MEF (<http://p300db.choudharylab.org>). Furthermore, ATG5 and ATG16L1, two proteins essential for the assembly of autophagosomes, exhibited CBP/ p300-dependent acetylation sites²¹. Whether proteasome and autophagy components are acetylated in a CBP- and p300-dependent manner in SF, remains to be functionally evaluated²¹. Since CBP/ p300-dependent acetylation sites in MEF were analyzed after a combinatorial knockout of both enzymes, it is not clear which of them is the major enzyme in regulating the post-translational acetylation of proteins involved in the regulation of autophagy and proteasome activities.

In summary, we have identified CBP and in particular p300 as pivotal regulators of stress response pathways in SF, with overlapping and distinct functions within specific pathways. The downregulation of p300 by TNF and oxidative stress provides a mechanism underlying SF activation in the synovial microenvironment.

Material and methods

Patient samples and cell preparation

Synovial tissue specimens were obtained from hand, shoulder and knee joints of RA patients undergoing joint replacement surgery (Schulthess Clinic Zurich, Switzerland)³². All patients fulfilled the criteria for the classification of RA³³. SF were isolated and cultured as described elsewhere⁷ and used between passages four and eight for all experiments. The study was conducted in accordance with the Declaration of Helsinki, and approved by the Cantonal Ethics Committee Zurich, Switzerland (approval numbers 2019–00,115 and 2019–00,674)³². Informed consent was obtained from all patients prior the inclusion into the study.

Silencing of CBP and p300

SF were transfected with antisense LNA gapmeRs targeting CBP, p300 or gapmeR control (Qiagen) using lipofectamine (Thermo Scientific) as described previously¹⁴. Twenty-four hours after transfection, cells were stimulated with TNF (10 ng/ml) for 24 h. Knockdown of CBP and p300 was verified by real-time PCR and Western blotting¹⁴.

RNA sequencing of SF

We have performed RNA sequencing (RNAseq) of SF (n = 6, with 3 cultures derived from hand and 3 from knee) silenced for CBP, p300 or controls in absence and presence of TNF (10 ng/ml). Experimental details on RNAseq have been published in our previous study¹⁴. RNAseq data have been deposited in NCBI's Gene Expression Omnibus³⁴ and are accessible through the GEO Series accession number GSE236122. Differentially expressed genes (DEG) entered pathway enrichment analysis using Gene Ontology (GO) terms and the "clusterProfiler" package of Bioconductor. Stress related pathways were selected by expert opinion to prepare customized graphs.

Real-time PCR

Total RNA was isolated using the RNeasy Mini Kit (Qiagen) including on-column DNaseI digest and was reversed transcribed³². Real-time PCR (7900HT real-time PCR system, Life Technologies) was performed using

self-designed primers (Microsynth, supplementary table 1) and SYBR green (Roche)³⁵. Dissociation curves and samples containing the untranscribed RNA were measured in parallel. Constitutively expressed human ribosomal protein large P0 (RPLP0) was measured for internal standard sample normalization and relative mRNA expression levels were calculated by the comparative threshold cycle method ($\Delta\Delta Ct$)³⁶.

Treatment of SF

For assessing effects on autophagy, SF were silenced for CBP or p300 and treated with TNF as described above. Bafilomycin A1 (100 nM, Tocris Bioscience) was added for 4 h prior to harvesting the cells. For assessing the regulation of CBP and p300 protein expression, SF were treated with TNF (10 ng/ml), 4-hydroxynonenal (4-HNE, 5 μ M, Sigma Aldrich), or a combination of both for 48 h, or with H₂O₂ (0,1 and 0,3 mM, Sigma Aldrich) for 24 h. Controls were treated with matched amounts of ethanol.

Western blotting

SF were lysed in Laemmli buffer (62.5 mM TrisHCl, 2% SDS, 10% glycerol, 0.1% bromphenolblue, 5 mM β -mercaptoethanol). Western blotting was performed as described previously³². In brief, whole cell lysates were separated on SDS polyacrylamide gels and electro blotted onto nitrocellulose membranes (Whatman). Membranes were blocked for 1 h in 5% (w/v) non-fat milk in TBS-T (20 mM Tris base, 137 mM sodium chloride, 0.1% Tween 20, pH 7.6). Membranes were cut in pieces covering different protein sizes prior hybridization with primary antibodies, enabling us to use the same membrane for detection of different proteins without stripping of the membranes. The membranes were probed with antibodies against CBP (Cell Signaling), p300 (abcam), light chain 3 B (LC3B; Cell Signaling), p62 (abcam), ubiquitin (Lys48; Millipore) or α -tubulin (abcam). We have tested the specificity of all antibodies previously^{5,14,29}. As secondary antibodies, horseradish peroxidase-conjugated goat anti-rabbit or goat anti-mouse antibodies (Jackson ImmunoResearch) were used. Signals were detected using the ECL Western blotting detection reagents (GE Healthcare) and the Alpha Imager Software system (Alpha Innotech). Band intensities were measured using the Alpha Imager Software, and band intensities were calculated relative to the expression of α -tubulin.

ELISA

VEGF was measured in cell culture supernatants using ELISA according to the manufacturer's instructions (R&D Systems).

Proteasome activity assay

SF were transfected and treated as described above. Proteasome activities were measured using the Proteasome-Glo 3-Substrate Cell Based Assay System (Promega) following the manufacturer's instructions.

Analysis of ChIPseq data sets

ChIPseq data sets for H3K27ac in hand, shoulder and knee SF were generated previously⁷ and are available at the GEO repository accession GSE163548³⁷. The presence of H3K27ac in genomic regions autophagy-related genes was visualized using the Integrative Genomics Viewer (IGV)³⁸.

Statistical analysis

Statistical analysis on data sets was carried out by using the GraphPad Prism Software as described previously³². N numbers in all experiments represent biological samples from different patients. Differences between experimental groups were analyzed by analysis of variance (ANOVA) followed by Tukey's multiple comparison test. Data that were not normally distributed, were analyzed by Friedmann test followed by the post hoc Dunn's multiple comparison test. Data are reported as means \pm standard deviations. P values < 0.05 were considered significant.

Data availability

The RNAseq data discussed in this publication have been deposited in NCBI's Gene Expression Omnibus³⁴ and are accessible through the GEO Series accession number GSE236122 (<https://www.ncbi.nlm.nih.gov/geo/query/acc.cgi?acc=GSE236122>). Other datasets used and/or analysed during the current study are available from the corresponding author on reasonable request.

Received: 6 September 2022; Accepted: 8 October 2023

Published online: 10 October 2023

References

1. Fearon, U., Canavan, M., Biniecka, M. & Veale, D. J. Hypoxia, mitochondrial dysfunction and synovial invasiveness in rheumatoid arthritis. *Nat. Rev. Rheumatol.* **12**, 385–397. <https://doi.org/10.1038/nrrheum.2016.69> (2016).
2. Yamasaki, S., Yagishita, N., Tsuchimochi, K., Nishioka, K. & Nakajima, T. Rheumatoid arthritis as a hyper-endoplasmic-reticulum-associated degradation disease. *Arthritis Res. Ther.* **7**, 181–186. <https://doi.org/10.1186/ar1808> (2005).
3. Zhu, L. *et al.* The autophagy level is increased in the synovial tissues of patients with active rheumatoid arthritis and is correlated with disease severity. *Mediators Inflamm.* **2017**, 7623145. <https://doi.org/10.1155/2017/7623145> (2017).
4. Shin, Y. J. *et al.* Autophagy induction and CHOP under-expression promotes survival of fibroblasts from rheumatoid arthritis patients under endoplasmic reticulum stress. *Arthritis Res. Ther.* **12**, R19. <https://doi.org/10.1186/ar2921> (2010).
5. Kato, M., Ospelt, C., Gay, R. E., Gay, S. & Klein, K. Dual role of autophagy in stress-induced cell death in rheumatoid arthritis synovial fibroblasts. *Arthritis Rheumatol.* **66**, 40–48. <https://doi.org/10.1002/art.38190> (2014).
6. Korb, A., Pavenstadt, H. & Pap, T. Cell death in rheumatoid arthritis. *Apoptosis* **14**, 447–454. <https://doi.org/10.1007/s10495-009-0317-y> (2009).

7. Frank-Bertoncelj, M. *et al.* Epigenetically-driven anatomical diversity of synovial fibroblasts guides joint-specific fibroblast functions. *Nat. Commun.* **8**, 14852. <https://doi.org/10.1038/ncomms14852> (2017).
8. Ospelt, C. Synovial fibroblasts in 2017. *RMD Open* **3**, e000471. <https://doi.org/10.1136/rmdopen-2017-000471> (2017).
9. Biniecka, M. *et al.* Dysregulated bioenergetics: A key regulator of joint inflammation. *Ann. Rheum. Dis.* **75**, 2192–2200. <https://doi.org/10.1136/annrheumdis-2015-208476> (2016).
10. Ng, C. T. *et al.* Synovial tissue hypoxia and inflammation in vivo. *Ann Rheum Dis.* **69**, 1389–1395. <https://doi.org/10.1136/ard.2009.119776> (2010).
11. Friscic, J. *et al.* The complement system drives local inflammatory tissue priming by metabolic reprogramming of synovial fibroblasts. *Immunity* **54**, 1002–1021. <https://doi.org/10.1016/j.immuni.2021.03.003> (2021).
12. Ramos, Y. F. *et al.* Genome-wide assessment of differential roles for p300 and CBP in transcription regulation. *Nucleic Acids Res* **38**, 5396–5408. <https://doi.org/10.1093/nar/gkq184> (2010).
13. Fauquier, L. *et al.* CBP and P300 regulate distinct gene networks required for human primary myoblast differentiation and muscle integrity. *Sci. Rep.* **8**, 12629. <https://doi.org/10.1038/s41598-018-31102-4> (2018).
14. Krosel, M. *et al.* Individual functions of the histone acetyl transferases CBP and p300 in regulating the inflammatory response of synovial fibroblasts. *J. Autoimmun.* **123**, 102709. <https://doi.org/10.1016/j.jaut.2021.102709> (2021).
15. Jin, Q. *et al.* Distinct roles of GCN5/PCAF-mediated H3K9ac and CBP/p300-mediated H3K18/27ac in nuclear receptor transactivation. *EMBO J.* **30**, 249–262. <https://doi.org/10.1038/emboj.2010.318> (2011).
16. Dancy, B. M. & Cole, P. A. Protein lysine acetylation by p300/CBP. *Chem. Rev.* **115**, 2419–2452. <https://doi.org/10.1021/cr500452k> (2015).
17. Uchida, K. 4-Hydroxy-2-nonenal: a product and mediator of oxidative stress. *Prog. Lipid Res.* **42**, 318–343. [https://doi.org/10.1016/s0163-7827\(03\)00014-6](https://doi.org/10.1016/s0163-7827(03)00014-6) (2003).
18. McGarry, T., Biniecka, M., Veale, D. J. & Fearon, U. Hypoxia, oxidative stress and inflammation. *Free Radic. Biol. Med.* **125**, 15–24. <https://doi.org/10.1016/j.freeradbiomed.2018.03.042> (2018).
19. Li, L., Tan, J., Miao, Y., Lei, P. & Zhang, Q. ROS and autophagy: interactions and molecular regulatory mechanisms. *Cell Mol. Neurobiol.* **35**, 615–621. <https://doi.org/10.1007/s10571-015-0166-x> (2015).
20. Calo, E. & Wysocka, J. Modification of enhancer chromatin: what, how, and why?. *Mol. Cell* **49**, 825–837. <https://doi.org/10.1016/j.molcel.2013.01.038> (2013).
21. Weinert, B. T. *et al.* Time-resolved analysis reveals rapid dynamics and broad scope of the CBP/p300 Acetylome. *Cell* **174**, 231–244. <https://doi.org/10.1016/j.cell.2018.04.033> (2018).
22. Loh, C. *et al.* TNF-induced inflammatory genes escape repression in fibroblast-like synoviocytes: Transcriptomic and epigenomic analysis. *Ann. Rheum. Dis.* **78**, 1205–1214. <https://doi.org/10.1136/annrheumdis-2018-214783> (2019).
23. Akgol, G. *et al.* Is 4-hydroxynonenal a predictive parameter for the development of joint erosion in patients with rheumatoid arthritis?. *Arch. Rheumatol.* **31**, 76–81. <https://doi.org/10.5606/ArchRheumatol.2016.5945> (2016).
24. Balogh, E. *et al.* Oxidative stress impairs energy metabolism in primary cells and synovial tissue of patients with rheumatoid arthritis. *Arthritis Res. Ther.* **20**, 95. <https://doi.org/10.1186/s13075-018-1592-1> (2018).
25. Connor, A. M., Mahomed, N., Gandhi, R., Keystone, E. C. & Berger, S. A. TNF α modulates protein degradation pathways in rheumatoid arthritis synovial fibroblasts. *Arthritis Res. Ther.* **14**, R62. <https://doi.org/10.1186/ar3778> (2012).
26. Lee, I. H. & Finkel, T. Regulation of autophagy by the p300 acetyltransferase. *J. Biol. Chem.* **284**, 6322–6328. <https://doi.org/10.1074/jbc.M807135200> (2009).
27. Xu, Y. & Wan, W. Acetylation in the regulation of autophagy. *Autophagy* **19**, 379–387. <https://doi.org/10.1080/15548627.2022.2062112> (2023).
28. Sun, J. *et al.* Acetylation modification during autophagy and vascular aging. *Front. Physiol.* **12**, 598267. <https://doi.org/10.3389/fphys.2021.598267> (2021).
29. Kato, M. *et al.* AAA-ATPase p97 suppresses apoptotic and autophagy-associated cell death in rheumatoid arthritis synovial fibroblasts. *Oncotarget* **7**, 64221–64232 (2016). <https://doi.org/10.18632/oncotarget.11890>
30. Chang, P., Li, H., Hu, H., Li, Y. & Wang, T. The role of HDAC6 in autophagy and NLRP3 inflammasome. *Front. Immunol.* **12**, 763831. <https://doi.org/10.3389/fimmu.2021.763831> (2021).
31. Hao, W. *et al.* Autophagy induction promoted by m(6)A reader YTHDF3 through translation upregulation of FOXO3 mRNA. *Nat. Commun.* **13**, 5845. <https://doi.org/10.1038/s41467-022-32963-0> (2022).
32. Krošel, M. *et al.* Bromodomain protein inhibitors reorganize the chromatin of synovial fibroblasts. *Cells* **12**, 1149 (2023).
33. Arnett, F. C. *et al.* The American rheumatism association 1987 revised criteria for the classification of rheumatoid arthritis. *Arthritis Rheum* **31**, 315–324 (1988).
34. Edgar, R., Domrachev, M. & Lash, A. E. Gene expression omnibus: NCBI gene expression and hybridization array data repository. *Nucleic Acids Res.* **30**, 207–210. <https://doi.org/10.1093/nar/30.1.207> (2002).
35. Klein, K. *et al.* The bromodomain protein inhibitor I-BET151 suppresses expression of inflammatory genes and matrix degrading enzymes in rheumatoid arthritis synovial fibroblasts. *Ann. Rheum. Dis.* **75**, 422–429. <https://doi.org/10.1136/annrheumdis-2014-205809> (2016).
36. Schmittgen, T. D. & Livak, K. J. Analyzing real-time PCR data by the comparative C(T) method. *Nat. Protoc.* **3**, 1101–1108. <https://doi.org/10.1038/nprot.2008.73> (2008).
37. Ge, X. *et al.* Functional genomics atlas of synovial fibroblasts defining rheumatoid arthritis heritability. *Genome Biol.* **22**, 247. <https://doi.org/10.1186/s13059-021-02460-6> (2021).
38. Thorvaldsdottir, H., Robinson, J. T. & Mesirov, J. P. Integrative genomics viewer (IGV): high-performance genomics data visualization and exploration. *Brief Bioinform.* **14**, 178–192. <https://doi.org/10.1093/bib/bbs017> (2013).

Acknowledgements

We thank Maria Comazzi, Peter Künzler and Matthias Brunner for excellent technical assistance. We thank Miriam Marks (Schulthess Klinik Zürich) for the collection of synovial tissues.

Author contributions

MK: Investigation, formal analysis, visualization, funding acquisition; MG: investigation, formal analysis, visualization; LM: investigation, formal analysis, visualization; MM: investigation, formal analysis, visualization; TZ: investigation, visualization; TS: investigation, visualization; MT: supervision, resources; OD: funding acquisition, supervision, resources; CO: supervision, resources; KK: conceptualization, methodology, supervision, resources, funding acquisition, writing- original draft preparation. All authors have critically reviewed the manuscript and agreed to the published version of the manuscript.

Funding

This work was supported by the Swiss National Foundation (PMPDP3-171315), the Foundation for Research in Science and the Humanities at the University of Zurich (STWF-10-004), the EMDO Foundation (1042) and the Novartis Foundation for medical-biological Research (19A036). MK received a scientific training bursary provided by EULAR.

Competing interests

The authors declare no competing interests.

Additional information

Supplementary Information The online version contains supplementary material available at <https://doi.org/10.1038/s41598-023-44412-z>.

Correspondence and requests for materials should be addressed to K.K.

Reprints and permissions information is available at www.nature.com/reprints.

Publisher's note Springer Nature remains neutral with regard to jurisdictional claims in published maps and institutional affiliations.



Open Access This article is licensed under a Creative Commons Attribution 4.0 International License, which permits use, sharing, adaptation, distribution and reproduction in any medium or format, as long as you give appropriate credit to the original author(s) and the source, provide a link to the Creative Commons licence, and indicate if changes were made. The images or other third party material in this article are included in the article's Creative Commons licence, unless indicated otherwise in a credit line to the material. If material is not included in the article's Creative Commons licence and your intended use is not permitted by statutory regulation or exceeds the permitted use, you will need to obtain permission directly from the copyright holder. To view a copy of this licence, visit <http://creativecommons.org/licenses/by/4.0/>.

© The Author(s) 2023